

JTRP

Joint
Transportation
Research
Program

FHWA/TN/JHRP-97/7

Summary Report

**RATED AXLE LOAD ENHANCEMENT
(RALE) SYSTEM**

**C. J. Lee
C. D. Sutton
T. D. White**

June 1997

Indiana
Department
of Transportation

Purdue
University

Summary Report

RATED AXLE LOAD ENHANCEMENT (RALE) SYSTEM

by

C. J. Lee
Graduate Assistant

C. D. Sutton
Associate Professor of Civil Engineering

T. D. White
Professor of Civil Engineering

Joint Highway Research Project
Project No.: C-36-37GG
File No.: 5-8-33

Prepared as Part of an Investigation
Conducted by

Joint Highway Research Project
Engineering Experiment Station
Purdue University

In cooperation with the

Indiana Department of Transportation
and the
U.S. Department of Transportation
Federal Highway Administration

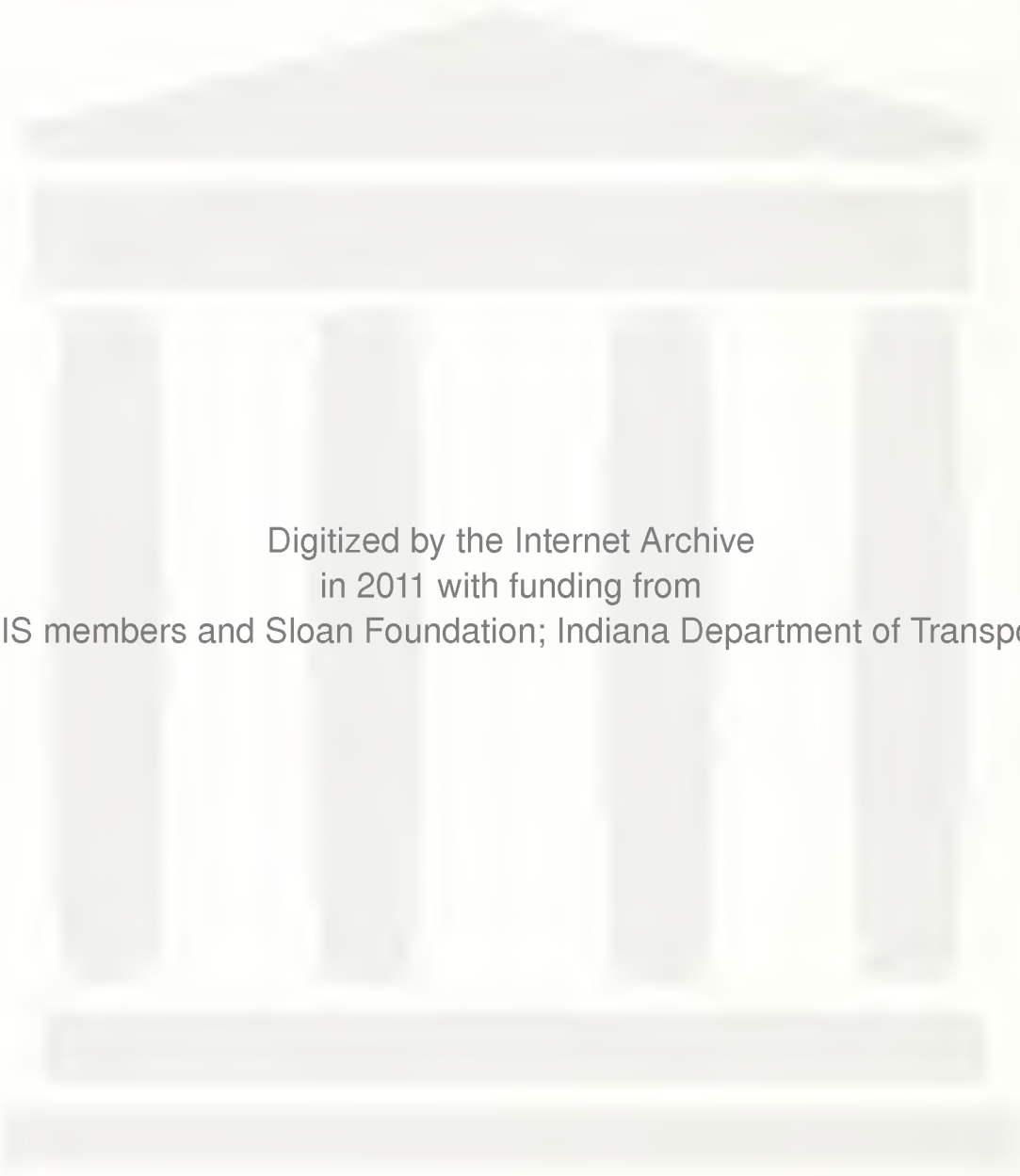
The contents of this report reflect the view of the authors, who are responsible for the facts and the accuracy of the data presented herein. The contents do not necessarily reflect the official views or policies of the Indiana Department of Transportation or the Federal Highway Administration at the time of publication. This report does not constitute a standard, specification or regulation.

Purdue University
West Lafayette, Indiana 47907

June 1997

TECHNICAL REPORT STANDARD TITLE PAGE

1. Report No. FHWA/IN/JTRP-97/7	2. Government Accession No.	3. Recipient's Catalog No.	
4. Title and Subtitle Rated Axle Load Enhancement (RALE) System		5. Report Date June 1997	
		6. Performing Organization Code	
7. Author(s) C. J. Lee, C. D. Sutton and T. White		8. Performing Organization Report No. FHWA/IN/JTRP-97/7	
9. Performing Organization Name and Address Joint Transportation Research Program 1284 Civil Engineering Building Purdue University West Lafayette, Indiana 47907-1284		10. Work Univ No.	
		11. Contract or Grant No. SPR-2160	
12. Sponsoring Agency Name and Address Indiana Department of Transportation State Office Building 100 North Senate Avenue Indianapolis, IN 46204		13. Type of Report and Period Covered Summary Report	
		14. Sponsoring Agency Code	
15. Supplementary Notes Prepared in cooperation with the Indiana Department of Transportation and Federal Highway Administration.			
16. Abstract <p>Concrete pavements in large part are designed as flat slabs although in the past they have included thickened edges. Thickened edge slabs are used today where positive load transfer for some reason can not be provided. The Rated Axle Load Enhancement (RALE) system concept involves the use of longitudinal stems to stiffen the concrete slab. A close analogy is that of a wide double or quadruple "T" beam. The stems may be rectangular or trapezoidal.</p> <p>In this study, RALE systems with two and four rectangular stems as well as plain concrete slabs were analyzed using the finite element method (FEM). The stresses in different pavement structures under wheel and thermal load were compared. The issue of curling/warping associated surface smoothness was also addressed. It is predicted that the RALE system would perform better than conventional flat slabs, especially for cases where thermal load is involved. In such cases, the RALE with four stems is better than the RALE with two stems.</p>			
17. Key Words concrete pavement, finite element method, thermal stress		18. Distribution Statement No restrictions. This document is available to the public through the National Technical Information Service, Springfield, VA 22161	
19. Security Classif. (of this report)	20. Security Classif. (of this page)	21. No. of Pages 39	22. Price



Digitized by the Internet Archive
in 2011 with funding from
LYRASIS members and Sloan Foundation; Indiana Department of Transportation

TABLE OF CONTENTS

	Page
ABSTRACT	iii
LIST OF FIGURES	iv
LIST OF TABLES	vi
INTRODUCTION	1
GEOMETRY	1
MATERIAL	2
LOADING	3
BOUNDARY CONDITIONS	4
REINFORCEMENT	4
RESULTS	5
CONCLUSIONS	8
REFERENCES	9

LIST OF FIGURES

- | | |
|-----------|--|
| Figure 1 | Geometry of RALE with two stems (stem size: 30.5 cm by 61 cm) |
| Figure 2 | Geometry of RALE with four stems (stem size: 15.2 cm by 61 cm) |
| Figure 3 | Deformed shapes of conventional flat slab system under -15°C thermal load |
| Figure 4 | Deformed shapes of conventional flat slab system under $+15^{\circ}\text{C}$ thermal load |
| Figure 5 | Deformed shapes of two stem RALE under -15°C thermal load |
| Figure 6 | Deformed shapes of complete two stem RALE system under -15°C thermal load |
| Figure 7 | Deformed shapes of two stem RALE under $+15^{\circ}\text{C}$ thermal load |
| Figure 8 | Deformed shapes of complete two stem RALE system under $+15^{\circ}\text{C}$ thermal load |
| Figure 9 | Deformed shape and stress contours of two stem RALE under wheel load |
| Figure 10 | Deformed shape and stress contours of two stem RALE under $+15^{\circ}\text{C}$ thermal load |
| Figure 11 | Deformed shape and stress contours of two stem RALE under -15°C thermal load |
| Figure 12 | Deformed shape and stress contours of two stem RALE under wheel and $+15^{\circ}\text{C}$ thermal load |
| Figure 13 | Deformed shape and stress contours of two stem RALE under wheel and -15°C thermal load |
| Figure 14 | Deformed shape and stress contours of four stem RALE under wheel load |
| Figure 15 | Deformed shape and stress contours of four stem RALE under $+15^{\circ}\text{C}$ thermal load |
| Figure 16 | Deformed shape and stress contours of four stem RALE under -15°C thermal load |

- Figure 17 Deformed shape and stress contours of four stem RALE under wheel and +15°C thermal load
- Figure 18 Deformed shape and stress contours of four stem RALE under wheel and -15°C thermal load
- Figure 19 Longitudinal profile of three pavement structures under -15°C temperature gradient
- Figure 20 Longitudinal profile of three pavement structures under +15°C temperature gradient
- Figure 21 Comparison of conventional flat slab with different four stem RALE systems under wheel load
- Figure 22 Comparison of conventional flat slab with different four stem RALE systems under +15C thermal load
- Figure 23 Comparison of conventional flat slab with different four stem RALE systems under -15C thermal load
- Figure 24 Comparison of conventional flat slab with different four stem RALE systems under wheel and thermal load +15C
- Figure 25 Comparison of conventional flat slab with different four stem RALE systems under wheel and thermal load -15C

LIST OF TABLES

Table 1	Parameters for each material used in the analysis
Table 2	Stress values of flat slabs with and without reinforcement
Table 3	Stress values of three cases consuming the same volume of concrete
Table 4	Stress ratio vs. allowable load repetitions

SPR-2160 Rated Axle Load Enhancement System

INTRODUCTION

An analysis was conducted to evaluate a stiffening concept for concrete pavements. Concrete pavements in large part are designed as flat slabs although in the past they have included thickened edges. Thickened edge slabs are used today where positive load transfer for some reason can not be provided. The Rated Axle Load Enhancement (RALE) system concept involves the use of longitudinal stems underneath the slab for stiffening. A close analogy is that of a wide double "T" beam. One or more stems may be utilized and the stems may be rectangular or trapezoidal.

In an initial study (Xue, 1996) [5] analysis was conducted of several stem configurations. The results indicated some benefit through reduction in stresses. This was encouraging because stress reductions of even a few percent can lead to significant improvement in pavement fatigue performance. It was recognized at the outset that stresses resulting from an environmental effect such as a temperature gradient should be considered. Current design criteria in the U.S. does not directly consider such restrained stresses.

The balance of this report provides details of the analysis and results obtained in the study.

GEOMETRY

In the first phase of this study, the finite element method (FEM) [1,2] was used to analyze the behavior of three pavement structures : a conventional flat slab, RALE

systems with two stems, and RALE systems with four stems. The concrete slab in all cases is 3.7 m wide and 6.1 m long. The thickness of the conventional flat slab is 35.6 cm while the thickness of all of the RALE surface slabs is 25.4 cm.

Only rectangular RALE stems were considered in the current study. In the two-stem RALE system, the stems are 30.5 cm wide and 61.0 cm deep as illustrated in Figure 1. The four-stem RALE system has stems that are 15.2 cm wide and 61.0 cm deep (Figure 2).

In all cases, the slabs are assumed to rest on a 20.3 cm aggregate subbase which is on a clay subgrade (CH) 2.0 m deep. The slabs are centered on the subbase/subgrade foundation which is 4.3 m wide and 6.7 m long. As a result, the stems are surrounded by the aggregate subbase to a depth of 20.3 cm. The remaining depth of the stem is surrounded by the clay subgrade. Deformed shapes of the flat slab and the two-stem RALE when subjected to minus and plus 15°C temperature loading are shown in Figures 3 through 8.

MATERIAL

A library of material models is available in the FEM software. Options from the library were utilized to model the concrete, subbase and subgrade materials. Since properties of concrete were well defined in the library model, the FEM material model “concrete” was used in the analysis. The subbase was represented as a Drucker-Prager elastic-plastic material and the subgrade was assumed to be a linear elastic material. Values for the key parameters of these material models are given in Table 1. This table also includes properties needed for the thermal analysis.

	Concrete	Subbase	Subgrade (CH)
Density (kg/m^3)	2400.	2200.	2000.
Modulus of Elasticity (Pa)	2.10E+10	1.38E+8	3.10E+7
Poisson's Ratio	0.15	0.4	0.4
Yield Stress (Pa)	1.84E+7	6.10E+5	1.25E+5
Ultimate stress (Pa)	3.20E+7.	(*)	(*)
Conductivity ($\text{W/m}^\circ\text{C}$)	1.298	(*)	(*)
Specific Heat ($\text{J/kg}^\circ\text{C}$)	879.2	795.5	711.8
Expansion Coefficient ($^\circ\text{C}$)	1.08E-5	(*)	(*)

(*) Values not needed in the analysis

Table 1 Parameters for each material used in the analysis

LOADING

Two types of loading, wheel and temperature loads, were considered in the analysis. Wheel loading consisted of a single 8,165 kg axle load on dual wheels. Tire pressure was assumed to be 689.5 kPa. Temperature loading was applied as a 15°C temperature differential both increasing and decreasing from the surface. Loading cases included :

1. Wheel load
2. Increasing temperature ($+15^\circ\text{C}$: 25°C at bottom of the slab and 40°C on top)
3. Decreasing temperature (-15°C : 15°C at bottom of the slab and 0°C on top)

4. Wheel load with increasing temperature
5. Wheel load with decreasing temperature

Temperature loading was applied as a gradient. The same finite element program used for the load analysis was used for the temperature analysis. Once the strain field from the temperature gradient is generated, the wheel loads can be imposed on the resulting strain field. Temperature gradients included in the analysis were 40°C (top) and 25°C (bottom) and 0°C (top) and 15°C (bottom).

BOUNDARY CONDITIONS

A condition of symmetry was assumed in the analysis. The planes of symmetry lie on all the four sides of subbase and subgrade. Bottom of the subgrade was assumed fixed. Between the top of the subbase and the bottom of the slab, a special element (contact element) was used to model the behavior of the interface and to provide a capability to visualize the gap between the two layers. This element was not used between subbase and subgrade because these two layers can be assumed continuous. In reality, opening or relative sliding between subbase and subgrade of concrete pavements seldom occurs.

REINFORCEMENT

A limited study was conducted on the effects of reinforcement. An analysis was made of the conventional flat slab and a four-stem RALE (stem size : 15.2 cm by 30 cm). In the conventional flat slab, No.3 rebars were assumed in both directions and at 12.7 cm below the top surface of the slab. A spacing of 15.2 cm was utilized. In the four-stem RALE,

two No.4 rebars were utilized in each stem. These two bars were located in the stems at 30.5cm and 45.7 cm below the bottom of the slab and were parallel to traffic.

RESULTS

The predicted, extreme values of the stresses are given in Table 2 and 3. In these tables S11 is the normal stress in the transverse direction (direction horizontal and perpendicular to traffic direction), S22 is the normal stress in the vertical direction and S33 is the normal stress in the longitudinal direction (direction horizontal and parallel to traffic direction). Of the three stresses, S22 is due mostly to the slab self weight and is less important. However, S11 and S33, can be tensile stresses. In Table 2, the stresses in the conventional flat slab with and without reinforcement are shown. As expected the effect of the reinforcement is insignificant (located near mid-depth). This reinforcement functions primarily as temperature steel and would become effective only when cracks occur. For comparison purposes, maximum stresses for the flat slab and two and four-stem RALE systems having the same cross section area are given in Table 3.

Based on stresses, the four-stem RALE with stem width of 15.2 cm performs better because the maximum tensile stresses under different loading conditions are generally the smallest among the three pavement structures.

In Figures 9 through 13, the deformed shapes and the stress contours of RALE systems with two stems under the five loading cases are plotted. Figure 9 shows the deformed shape and stress contours when the pavement is subjected to wheel load only. Figure 10 and 11 show results of thermal load ($\pm 15^{\circ}\text{C}$ respectively) only. Figure 12 and 13

show stresses resulting from the combined wheel and thermal loads. Similar results for four-stem RALE systems are shown in Figure 14 to Figure 18.

Temperature and/or moisture gradients cause either a convex or concave shape of the pavement surface to develop depending on if the gradient is negative or positive. To examine the magnitude and any difference from this effect, a longitudinal profile for the flat slab and two and four-stem RALEs (stem size of two-stem RALE is 30.5 cm by 61.0 cm and that of four-stem RALE is 15.2 cm by 61.0cm) with a plus and minus 15°C thermal load are shown in Figures 19 and 20, respectively. The joints between the slabs are fully efficient, that is, the load transfer ratio was assumed to be one hundred percent. These results indicate the RALE system would have less roughness. Less roughness translates into better pavement performance.

Figure 21 through Figure 25 compare results for the conventional flat slab with different four-stem RALE systems for five loading cases. The RALE systems have lower stresses than the conventional flat slab.

Evaluation of potential RALE system performance has to be done on a relative basis. The most obvious comparison is through performance relations for flat pavement slabs. Two methods for performance evaluation were utilized. Both essentially use the stress ratio to predict performance. The stress ratio is a ratio of cyclic tensile stress to the extreme fiber tensile stress at failure (modulus of rupture) of a beam tested in flexure. The higher the applied cyclic stress, the lower the number of cycles to fatigue failure of the beam. This model of concrete performance is used as an analogy for performance of concrete pavements subjected to repetitive loading.

The Portland Cement Association (PCA) [6] published a table of allowable repetitions for stress ratios ranging from 0.51 to 0.85 (see Table 4). An important characteristic implied by this data is that if the extreme fiber stress does not exceed 50 percent of the modulus of rupture then a concrete beam (or plain concrete pavement) will sustain a large (infinite) number of stress repetitions. The Portland Cement Association's concrete pavement design criteria utilizes this model for fatigue analysis.

In application of the fatigue model to performance evaluation of the RALE system a modulus of rupture had to be selected. The selected modulus of rupture was 3.09 MPa. This magnitude of modulus of rupture is low compared to current, representative values of modulus of rupture, but not unreasonable. More importantly, this choice of modulus of rupture places the resulting stress ratios for both the flat slab and RALE systems within the range of stress ratio values given in Table 4.

Using this value of modulus of rupture for a relative comparison of performance, the maximum tensile S11 stress of both the conventional flat slab and the four stem RALE (stem size : 15.2 cm by 61.0 cm) for a combined wheel load and minus temperature gradient (0°C surface temperature) are compared (Table 3). The flat slab S11 stress is 304.58 psi and that of the four stem RALE is 279.92 psi. These stresses produce stress ratios of 0.68 and 0.62. From Table 4, the allowable repetitions are 3,500 and 18,000, respectively. This is a relative result and the stresses include both thermal and wheel loads.

As an alternative analysis, an expression developed from analysis of the American Association of Highway Officials (AASHO) Road Test was utilized [7]. This expression includes the inverse stress ratio and is:

$$N_f = 225,000 \left(\frac{MR}{\sigma} \right)^4$$

where

MR = Modulus of Rupture

σ = Applied stress

N_f = Number of standard axles

Using the same modulus of rupture value (3.09 MPa) and stresses, the number of predicted standard axles for the flat slab and four-stem RALE are 1,080,000 and 1,523,000, respectively. Vesic's relation [7] is an empirical relation that includes both thermal and wheel loads at the AASHO Road Test. The design modulus of rupture used by the Indiana Department of Transportation is 4.46 MPa. Using this value results in N_f values of 6,629,000 and 4,703,000 for the RALE system and conventional slab, respectively.

CONCLUSIONS

Based on the results shown above, the following conclusions can be drawn:

1. Stresses are reduced in RALE systems.
2. There are high stress concentrations in some RALE geometries. However, these can be minimized by modification of the stem geometry.
3. Longitudinal roughness resulting from temperature loading can be less for RALE systems than for conventional flat slabs.

REFERENCES

1. ABAQUS/Standard 1994, User's Manual, Version 5.4, Hibbitt, Karlsson and Sorensen, Inc.
2. ABAQUS/Post 1994, User's Manual, Version 5.4-1, Hibbitt, Karlsson and Sorensen, Inc.
3. PATRAN3 On-line Help, 1995, MSC/PATRAN Products, MacNeal-Schwendler Corporation.
4. Huang, H. M., 1995, "Analysis of Accelerated Pavement Tests and Finite Element Modeling of Rutting Phenomenon", Ph.D Thesis, Purdue University.
5. Xue, F., 1996, "A study of Pavement Cross Section Geometry Using ABAQUS", M.S. Thesis, Purdue University
6. Portland Cement Association, "Thickness Design for Concrete Pavement," Portland Cement Association, 1966
7. Vesic, A. S. and L. Domaschuk, "Theoretical Analysis of Structural behavior of Road Test Flexible Pavements," Highway Research Board, NCHRP Report 10, 1966

Flat Slab (14" thick)

	Wheel Load	Wheel Load and 40C Surface Temp.	Wheel Load and 0C Surface Temp.	40C Surface Temp.	0C Surface Temp.
S11(Max. Comp.)	-21.76	-366.94	-122.85	-364.04	-122.56
S11(Max. Tension)	21.47	139.38	304.58	139.53	285.72
S22(Max.Comp.)	-25.53	-350.99	-119.66	-350.99	-114.72
S22(Max.Tension)	14.42	134.88	342.29	134.74	314.73
S33(Max. Comp.)	-71.5	-472.82	-122.12	-407.55	-106.31
S33(Max. Tension)	70.49	197.25	303.13	140.54	291.52

Flat Slab (14" thick, reinforced with No.3 rebars)

	Wheel Load	Wheel Load and 40C Surface Temp.	Wheel Load and 0C Surface Temp.	40C Surface Temp.	0C Surface Temp.
S11(Max. Comp.)	-21.61	-384.35	-126.47	-381.45	-127.63
S11(Max. Tension)	21.47	125.6	304.58	125.75	288.62
S22(Max.Comp.)	-25.38	-352.44	-120.96	-352.44	-114.29
S22(Max.Tension)	14.39	136.19	342.29	136.04	316.18
S33(Max. Comp.)	-71.07	-487.32	-126.62	-424.96	-109.94
S33(Max. Tension)	70.63	188.55	303.13	129.37	298.78

* All numbers are in units of psi.

** Numbers with a "-" sign are compressive stresses, "+" are tensile stresses.

Table 2 Stress values of flat slabs with and without reinforcement

Flat Slab (14" thick)

	Wheel Load	Wheel Load and 40C Surface Temp.	Wheel Load and 0C Surface Temp.	40C Surface Temp.	0C Surface Temp.
S11(Max. Comp.)	-21.76	-366.94	-122.85	-364.04	-122.56
S11(Max. Tension)	21.47	139.38	304.58	139.53	285.72
S22(Max.Comp.)	-25.53	-350.99	-119.66	-350.99	-114.72
S22(Max.Tension)	14.42	134.88	342.29	134.74	314.73
S33(Max. Comp.)	-71.5	-472.82	-122.12	-407.55	-106.31
S33(Max. Tension)	70.49	197.25	303.13	140.54	291.52

RALE with Two Stems (Stem Size : 1' by 2')

	Wheel Load	Wheel Load and 40C Surface Temp.	Wheel Load and 0C Surface Temp.	40C Surface Temp.	0C Surface Temp.
S11(Max. Comp.)	-23.21	-343.74	-156.64	-339.39	-147.94
S11(Max. Tension)	17.26	112.98	303.13	112.4	327.78
S22(Max.Comp.)	-31.62	-336.49	-142.14	-319.08	-134.88
S22(Max.Tension)	10.33	111.97	316.18	112.26	301.68
S33(Max. Comp.)	-49.02	-459.77	-109.94	-423.51	-119.37
S33(Max. Tension)	75.71	159.54	287.17	159.54	321.98

RALE with Four Stems (Stem Size : 1/2' by 2')

	Wheel Load	Wheel Load and 40C Surface Temp.	Wheel Load and 0C Surface Temp.	40C Surface Temp.	0C Surface Temp.
S11(Max. Comp.)	-31.18	-365.49	-175.49	-359.69	-165.34
S11(Max. Tension)	28.57	112.98	279.92	112.84	265.42
S22(Max.Comp.)	-28.72	-335.04	-116.32	-319.08	-105.44
S22(Max.Tension)	10.12	116.61	301.68	115.01	275.57
S33(Max. Comp.)	-48.88	-467.02	-163.89	-419.16	-158.09
S33(Max. Tension)	72.66	156.64	291.52	156.64	275.57

* All numbers are in units of psi.

** Numbers with a "-" sign are compressive stresses, "+" are tensile stresses.

Table 3 Stress values of three cases consuming the same volume of concrete

Stress Ratio	Allowable Repetition	Stress Ratio	Allowable Repetition
0.51	400,000	0.69	2,500
0.52	300,000	0.70	2,000
0.53	240,000	0.71	1,500
0.54	180,000	0.72	1,100
0.55	130,000	0.73	850
0.56	100,000	0.74	650
0.57	75,000	0.75	490
0.58	57,000	0.76	360
0.59	42,000	0.77	270
0.60	32,000	0.78	210
0.61	24,000	0.79	160
0.62	18,000	0.80	120
0.63	14,000	0.81	90
0.64	11,000	0.82	70
0.65	8,000	0.83	50
0.66	6,000	0.84	40
0.67	4,500	0.85	30
0.68	3,500		

Table 4 Stress ratio vs. allowable load repetitions

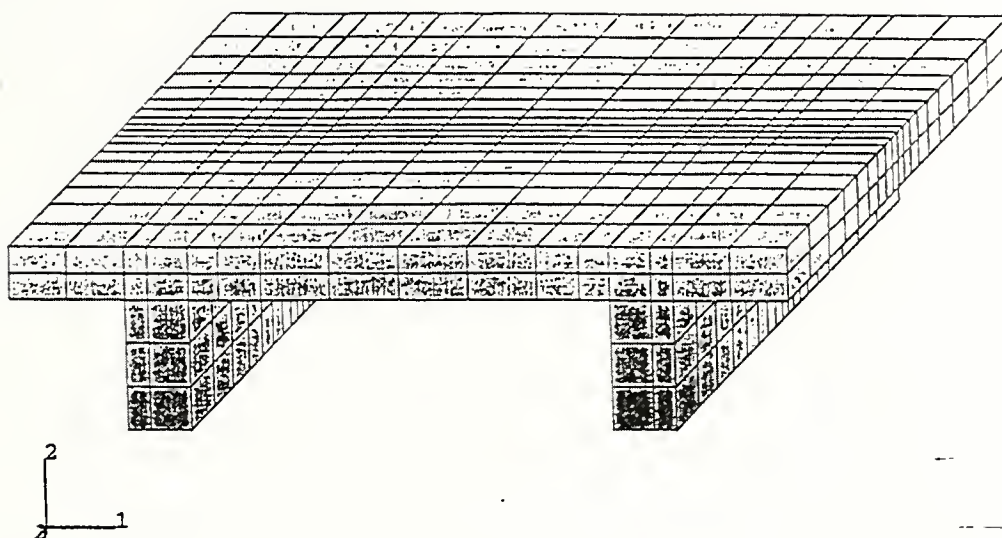


Figure 1 Geometry of RALE with two stems (stem size : 30.5 cm by 61 cm)

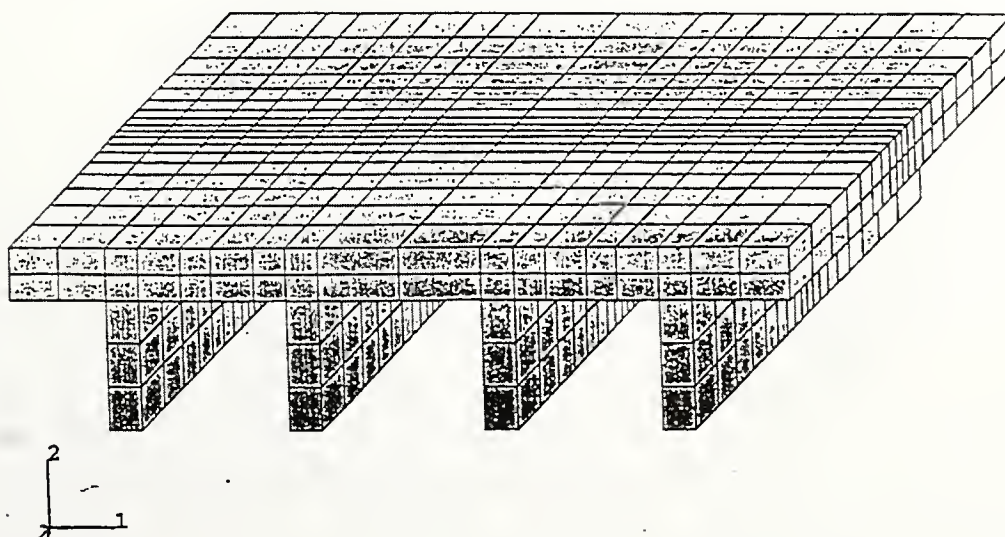


Figure 2 Geometry of RALE with four stems (stem size : 15.2 cm by 61 cm)

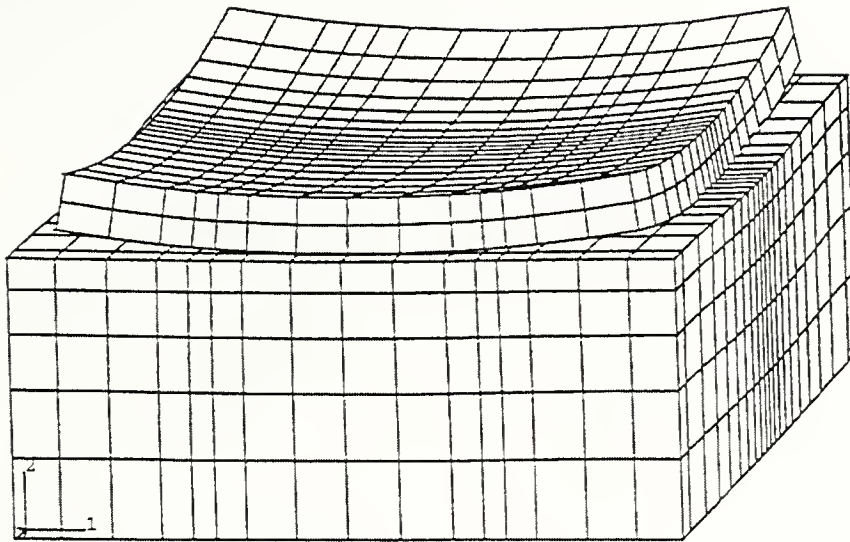


Figure 3 Deformed shapes of conventional flat slab system under -15°C thermal load

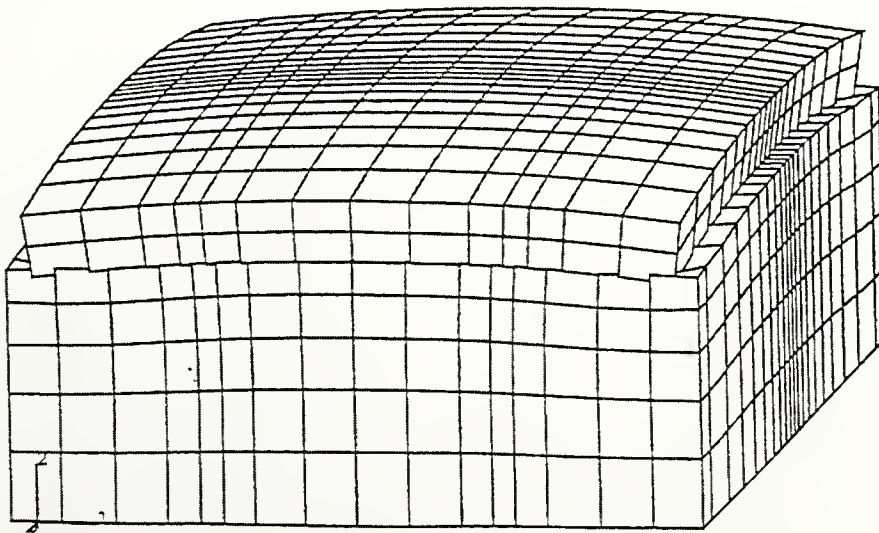


Figure 4 Deformed shapes of conventional flat slab system under +15°C thermal load

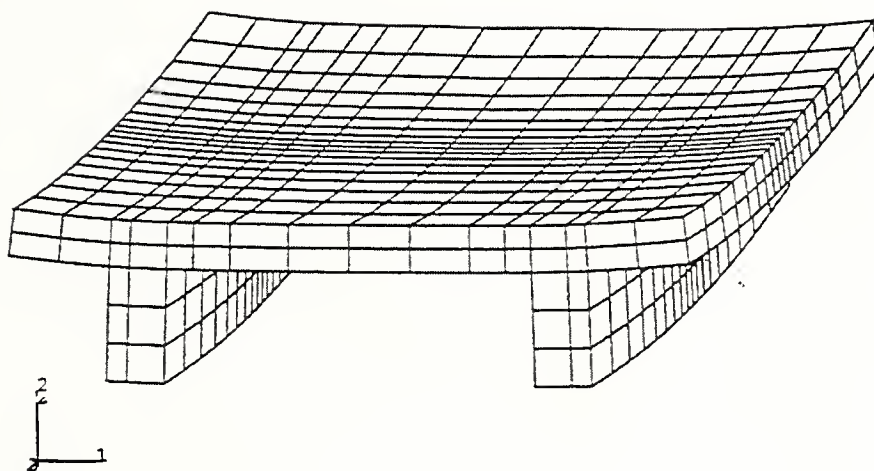


Figure 5 Deformed shapes of two stem RALE under -15°C thermal load

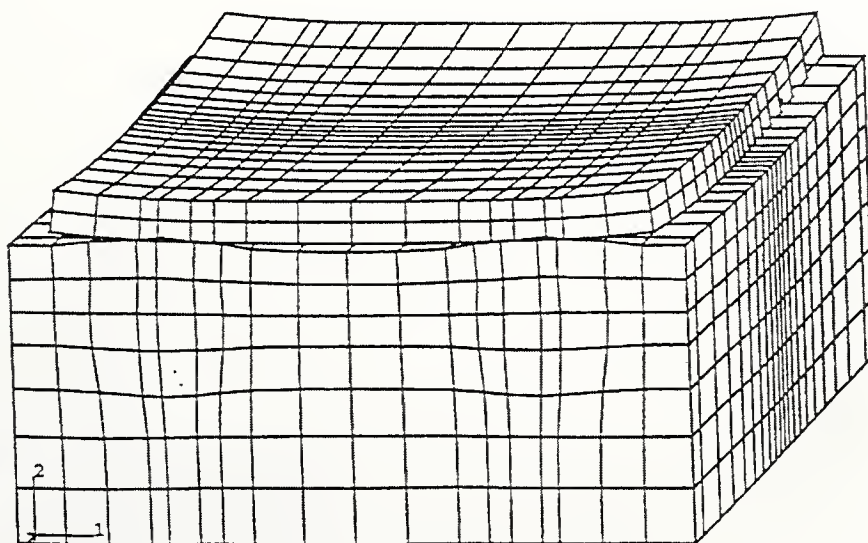


Figure 6 Deformed shapes of complete two stem RALE system under -15°C thermal load

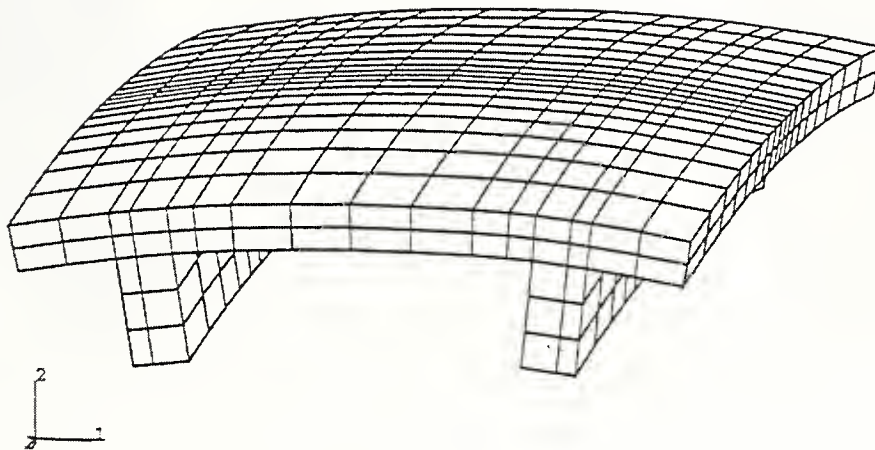


Figure 7 Deformed shapes of two stem RALE under $+15^{\circ}\text{C}$ thermal load

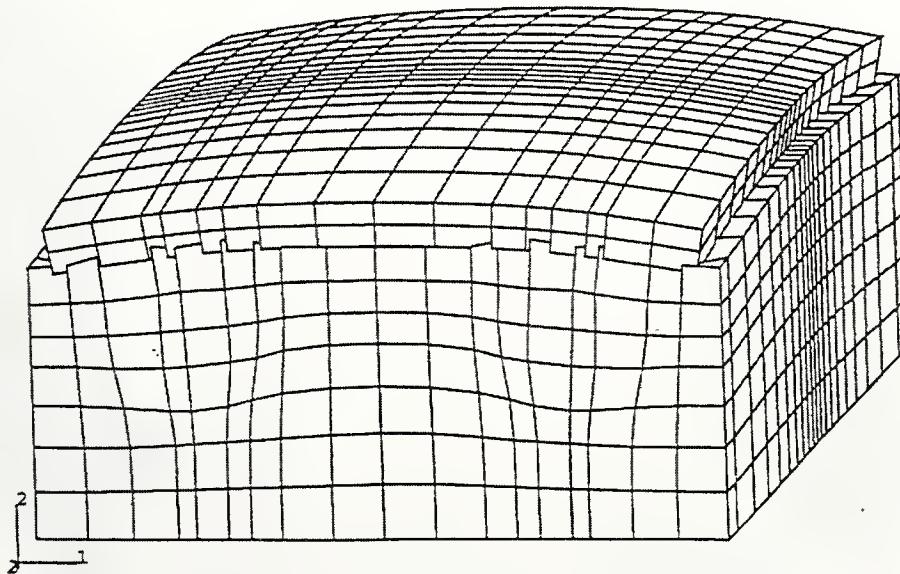


Figure 8 Deformed shapes of complete two stem RALE system under $+15^{\circ}\text{C}$ thermal load

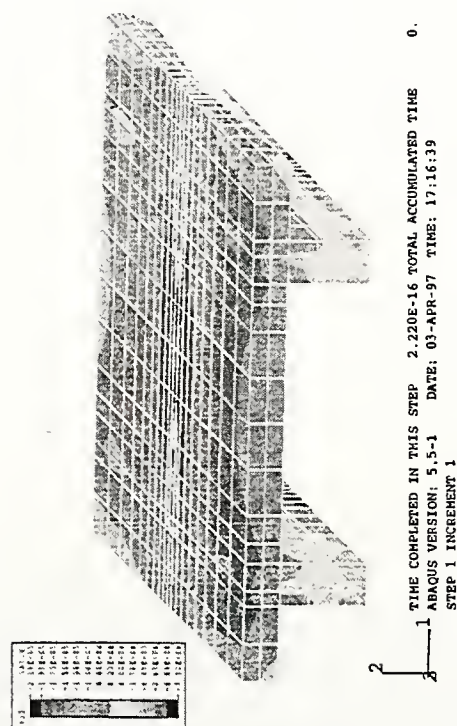
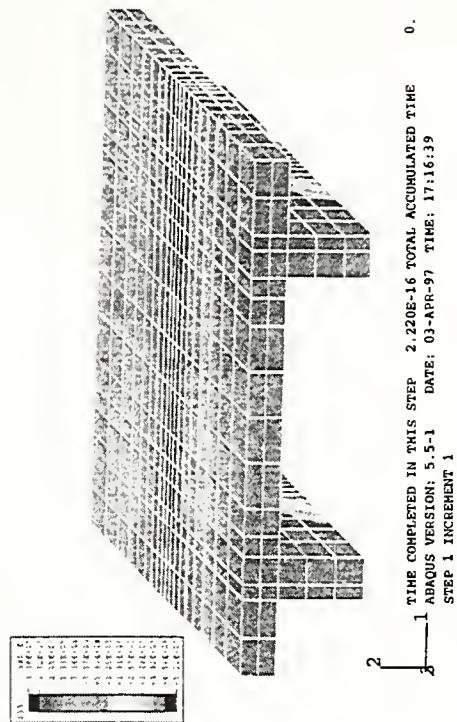
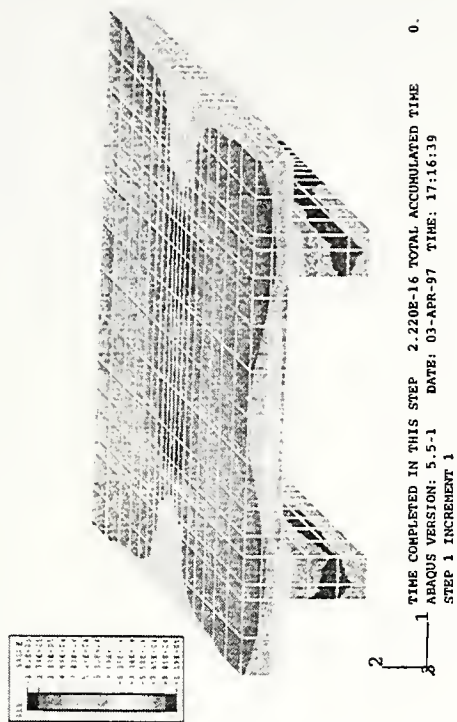


Figure 9 Deformed shape and stress contours of two stem RALE under wheel load

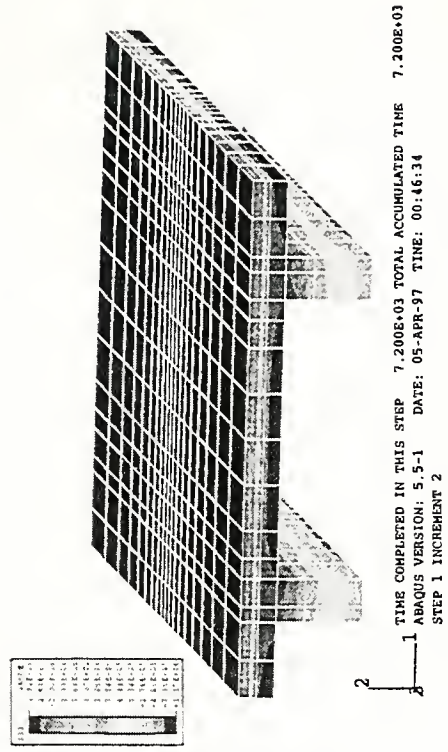
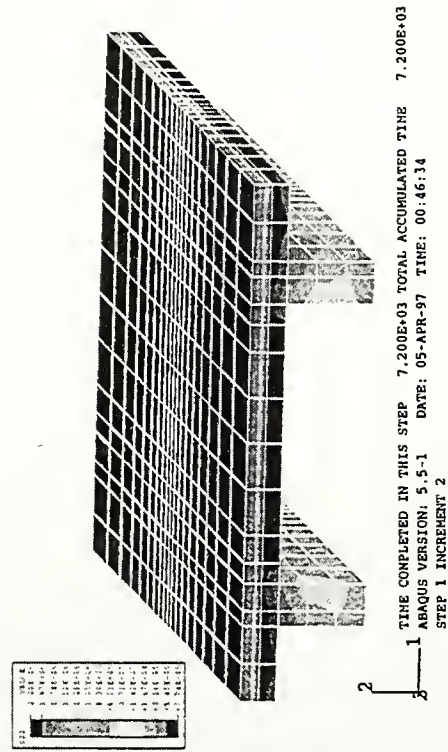
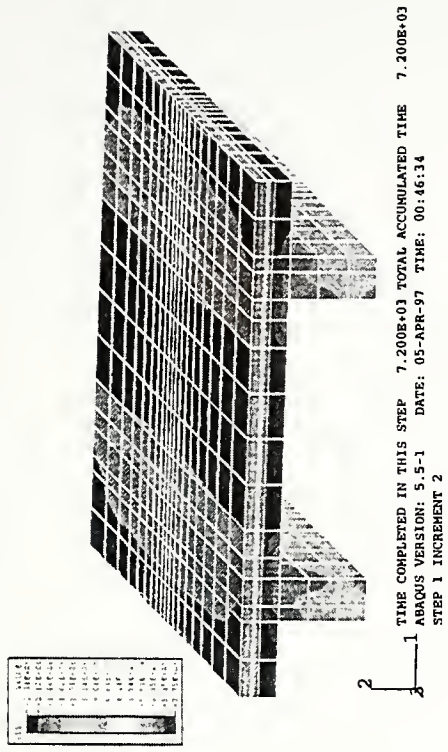


Figure 10 Deformed shape and stress contours of two stem RALE under +15°C thermal load

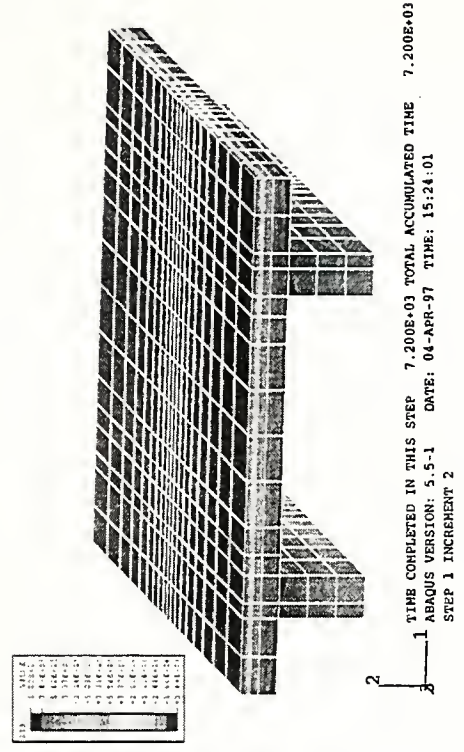
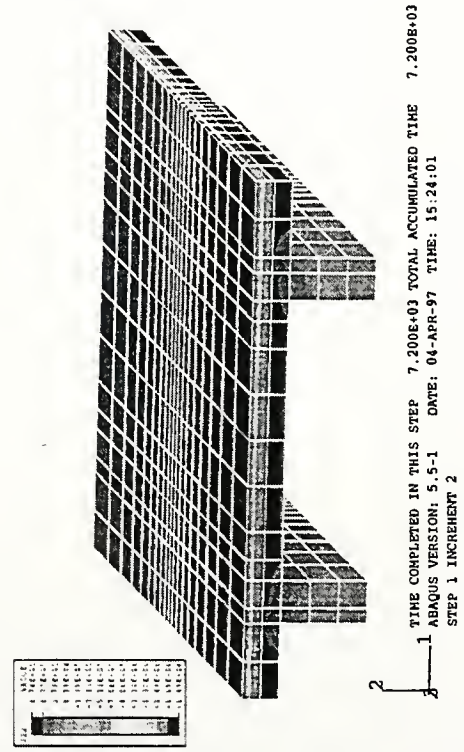
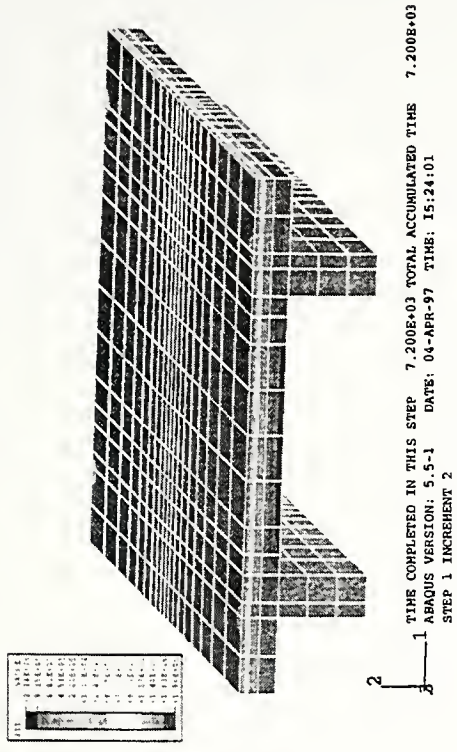


Figure 11 Deformed shape and stress contours of two stem RALE under -15°C thermal load

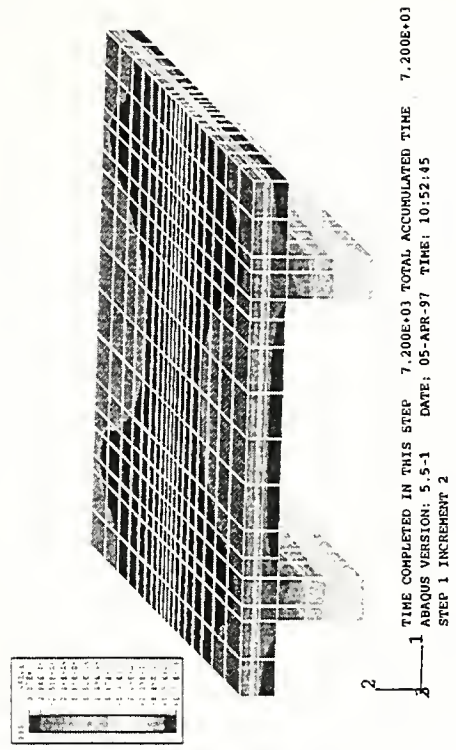
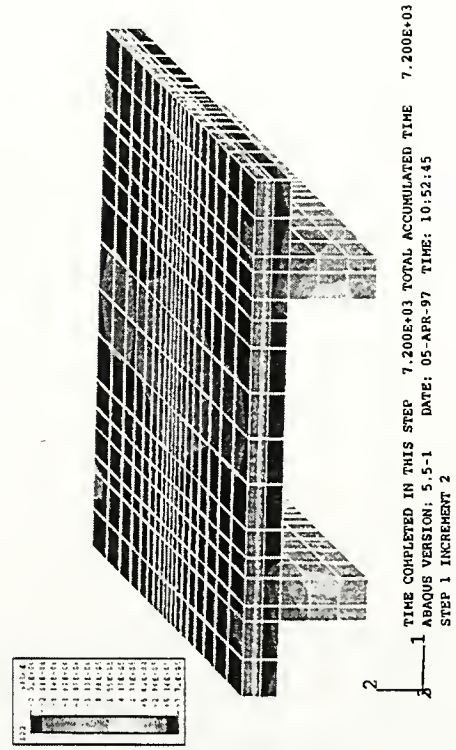
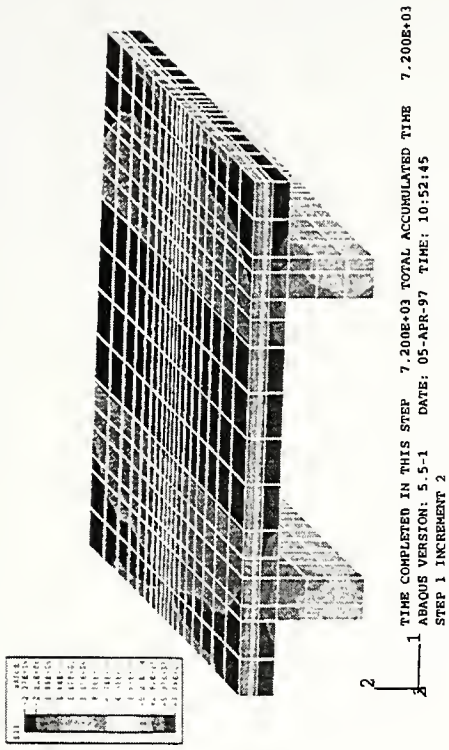


Figure 12 Deformed shape and stress contours of two stem RALE under wheel and +15°C thermal load

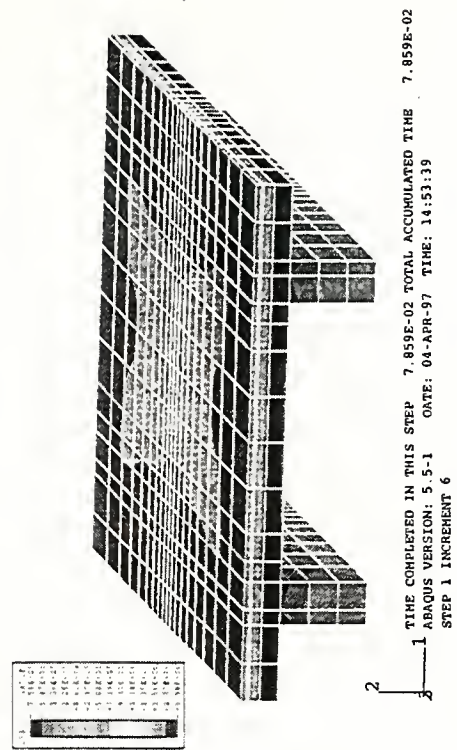
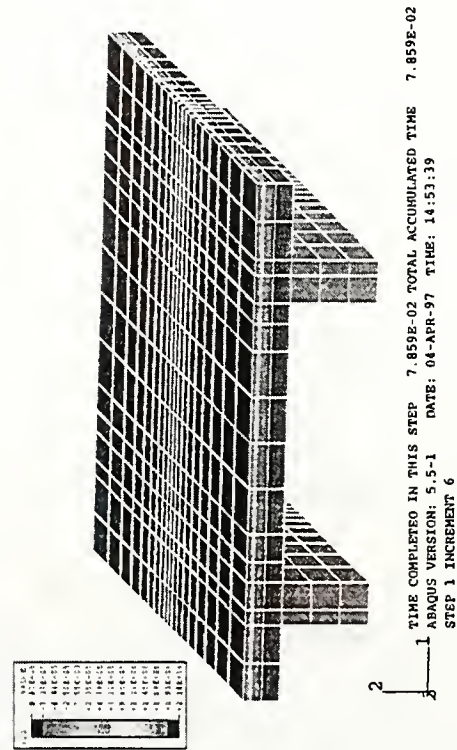
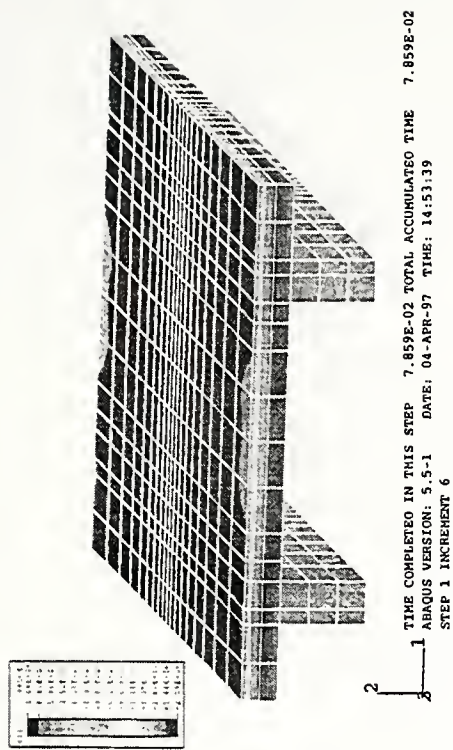
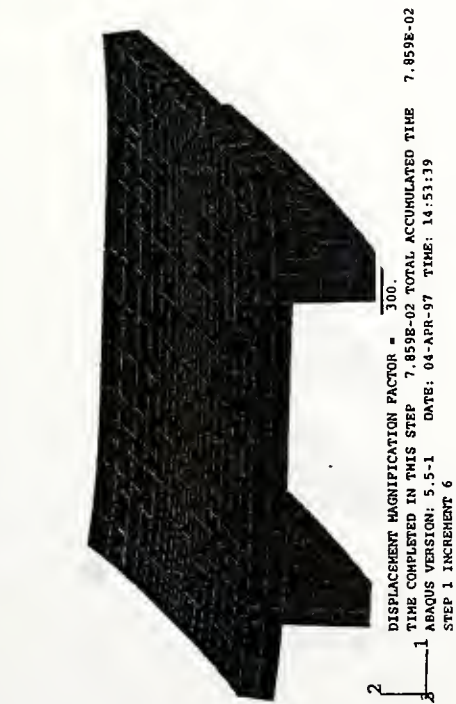


Figure 13 Deformed shape and stress contours of two stem RALE under wheel and -15°C thermal load

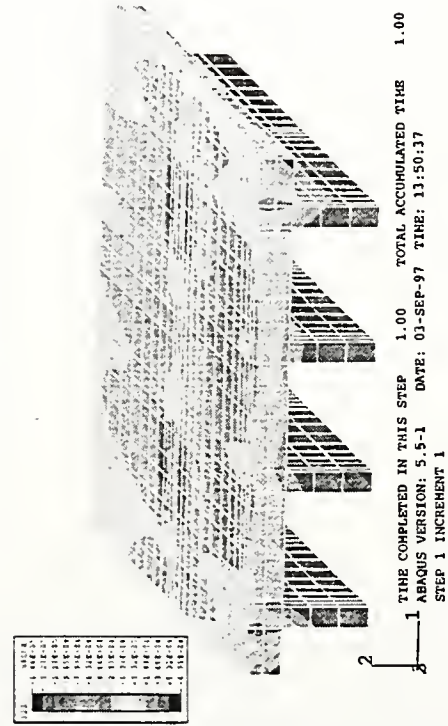
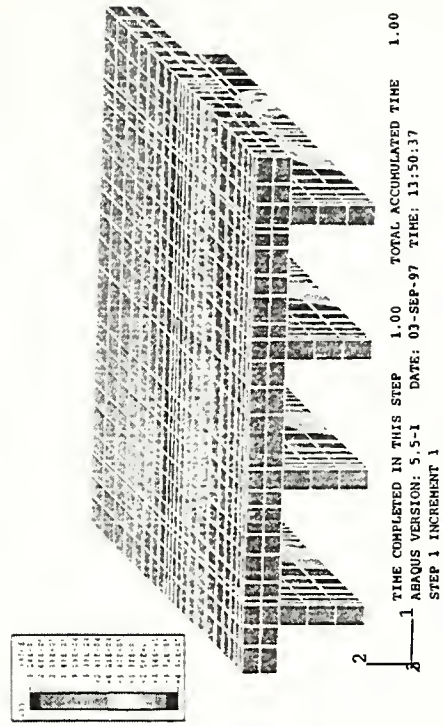
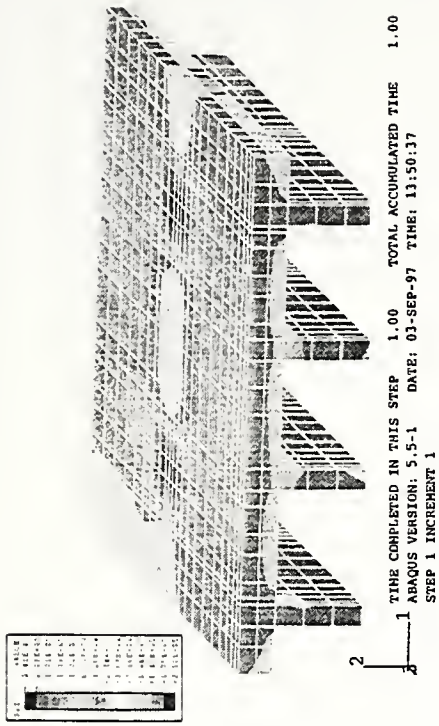


Figure 14 Deformed shape and stress contours of four stem RALE under wheel load

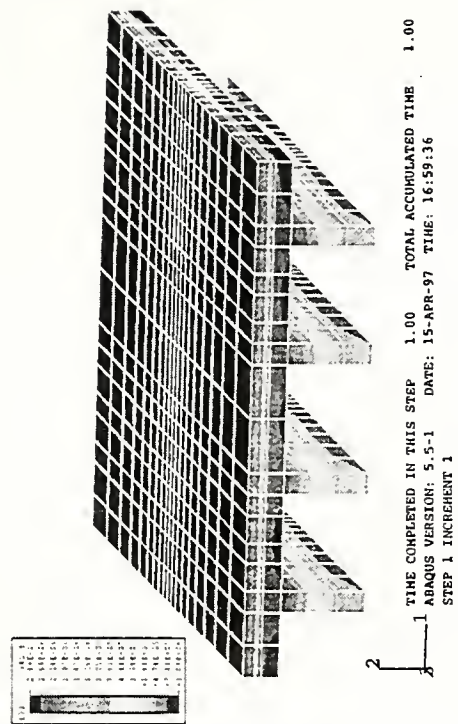
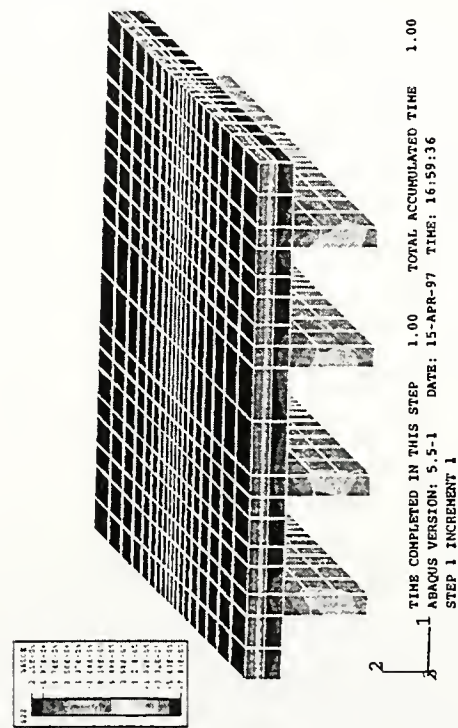
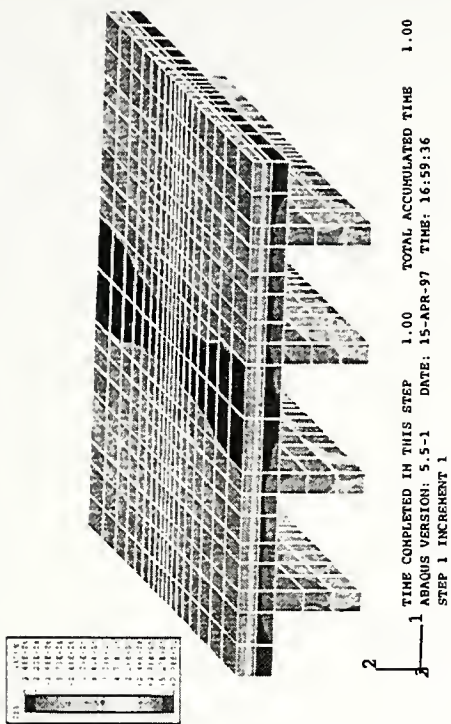


Figure 15 Deformed shape and stress contours of four stem RALE under +15°C thermal load

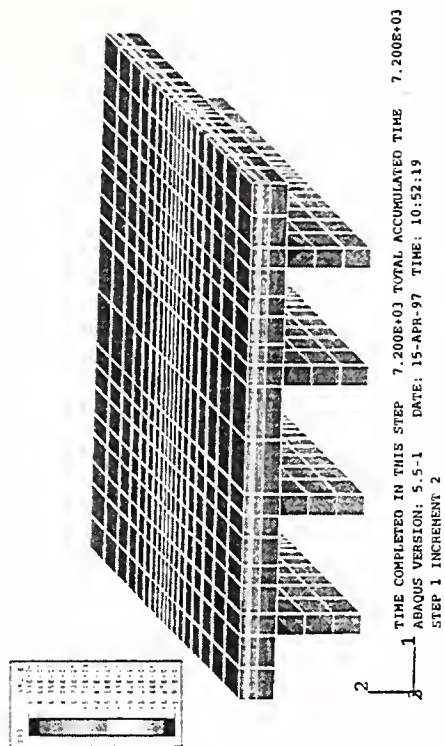
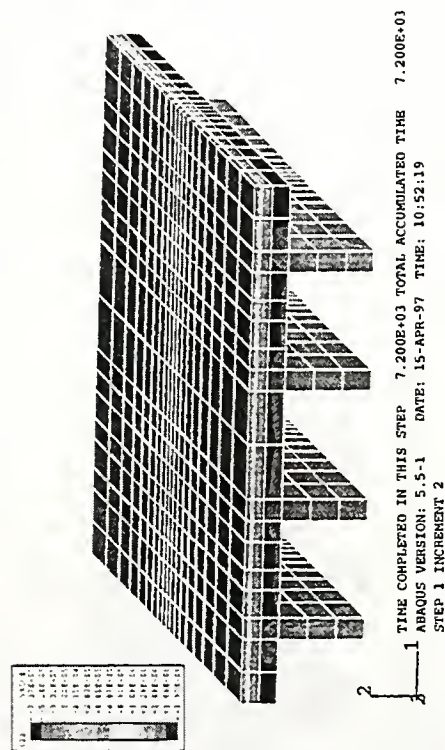
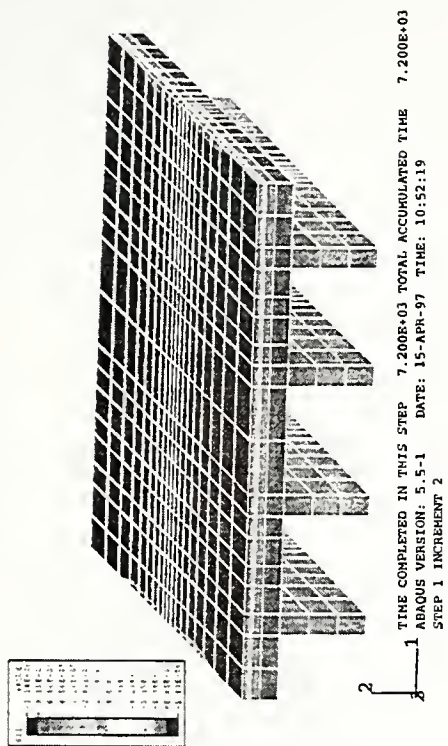


Figure 16 Deformed shape and stress contours of four stem RALJE under -15°C thermal load

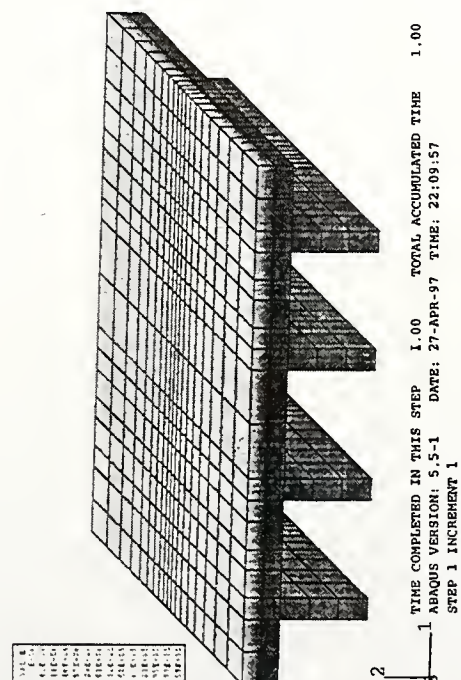
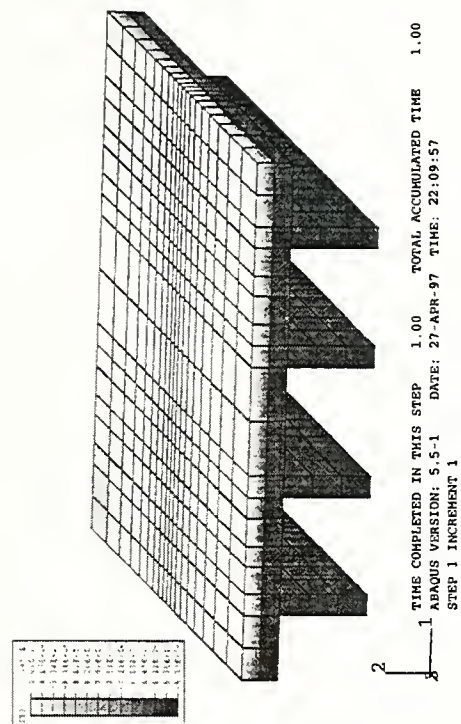
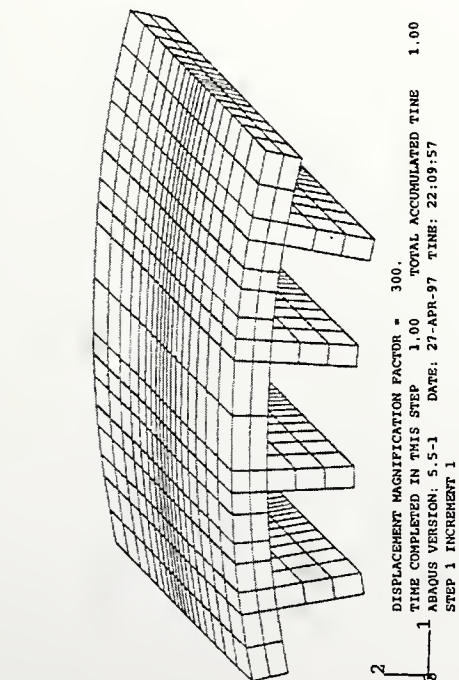
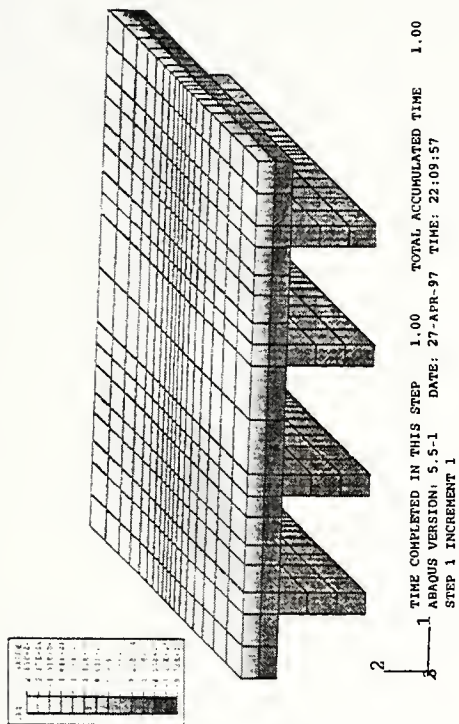


Figure 17 Deformed shape and stress contours of four stem RALE under wheel and +15°C thermal load

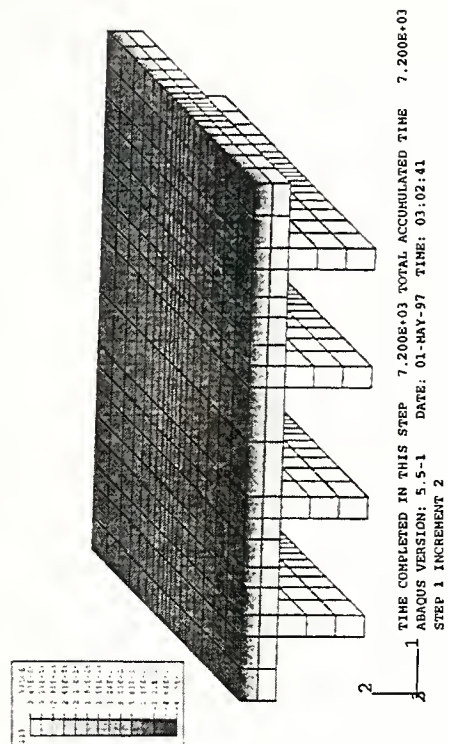
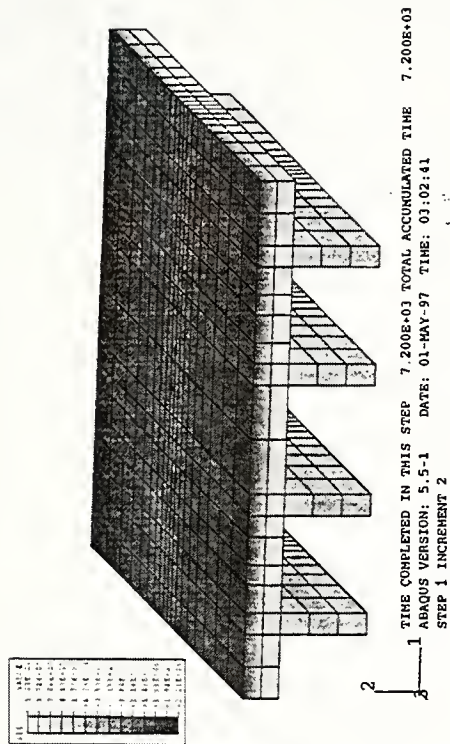


Figure 18 Deformed shape and stress contours of four stem RALE under wheel and -15°C thermal load

Longitudinal Profile under -15C Temperature Loading

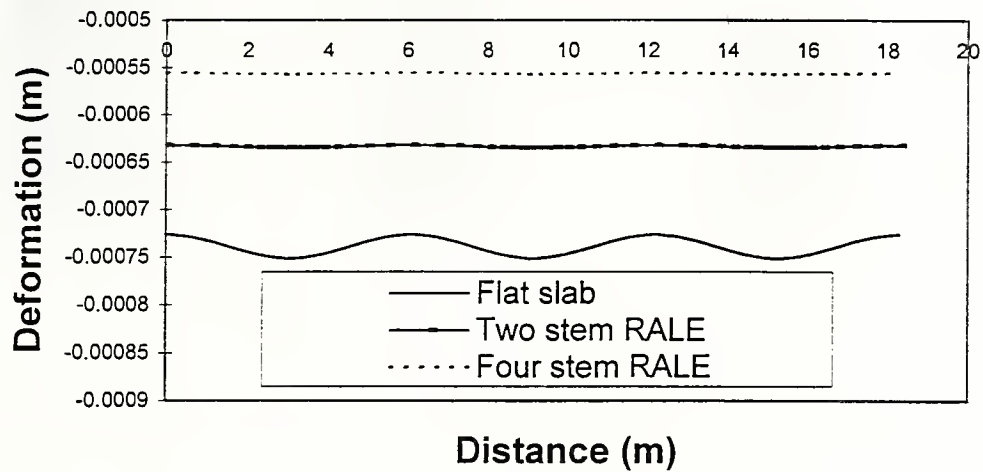


Figure 19 Longitudinal profile of three pavement structures under -15°C temperature gradient

Longitudinal Profile under +15C Temperature Loading

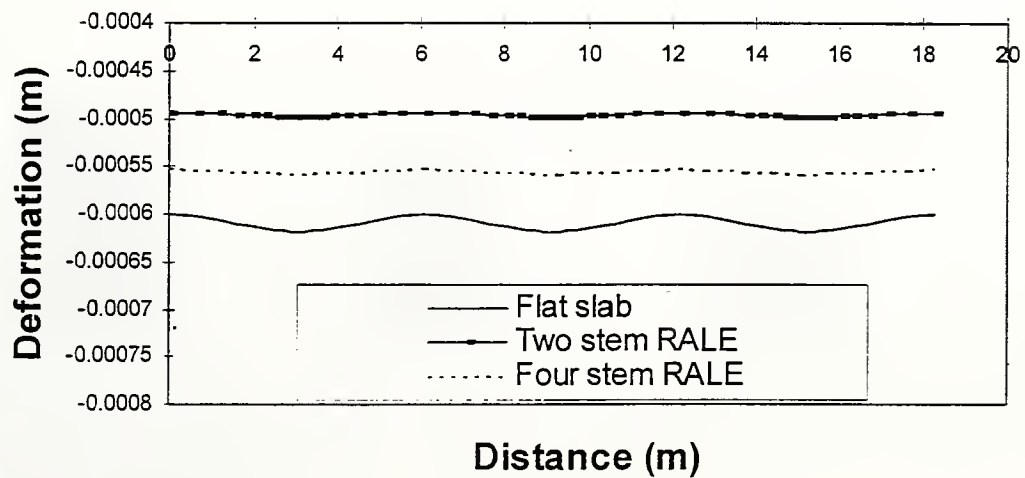


Figure 20 Longitudinal profile of three pavement structures under +15°C temperature gradient

Comparison of Flat Slab with Different Four Stem RALE Systems Under Wheel Load

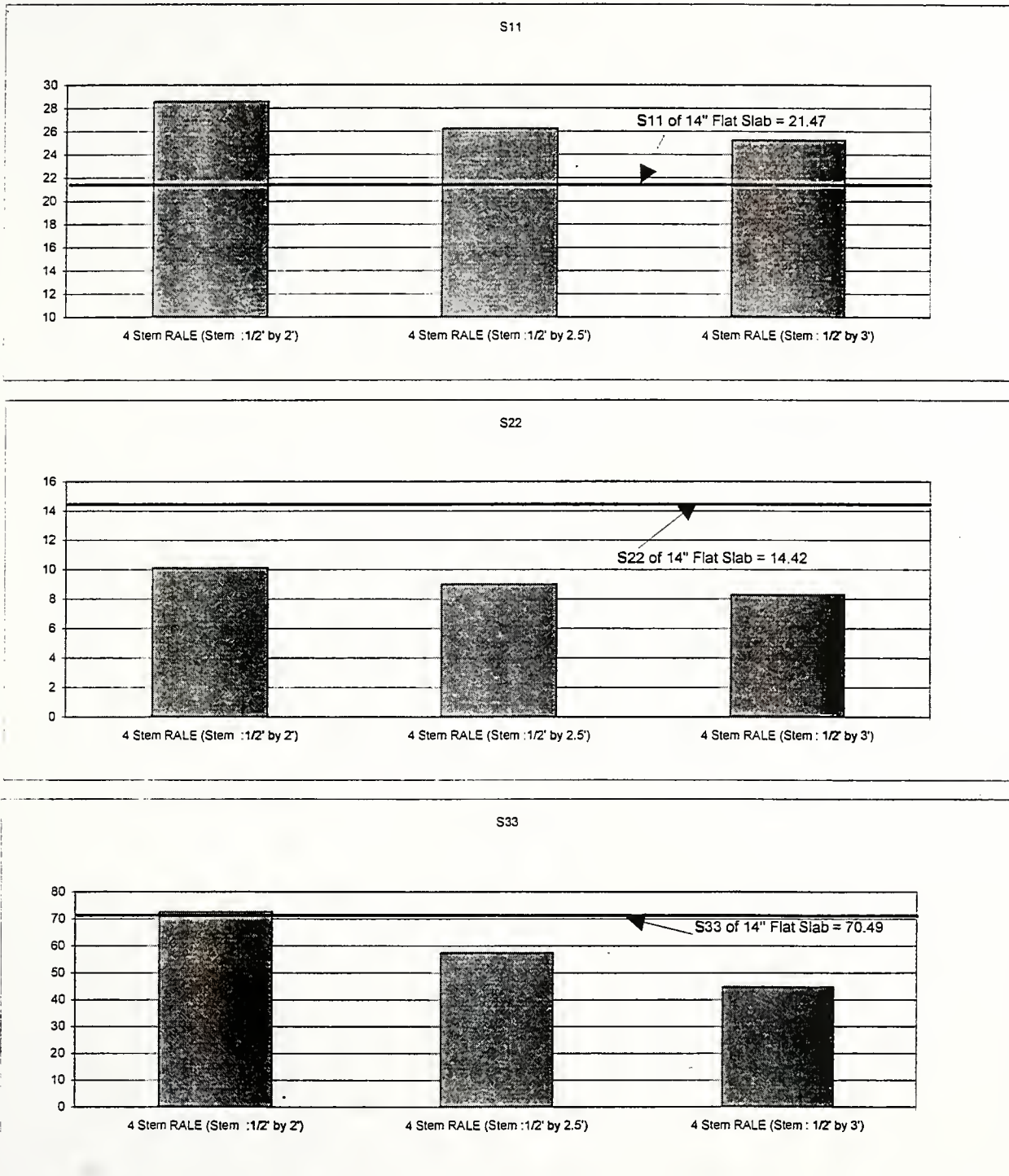


Figure 21 Comparison of conventional flat slab with different four stem RALE systems under wheel load

Comparison of Flat Slab with Different Four Stem RALE Systems Under +15C Thermal Load

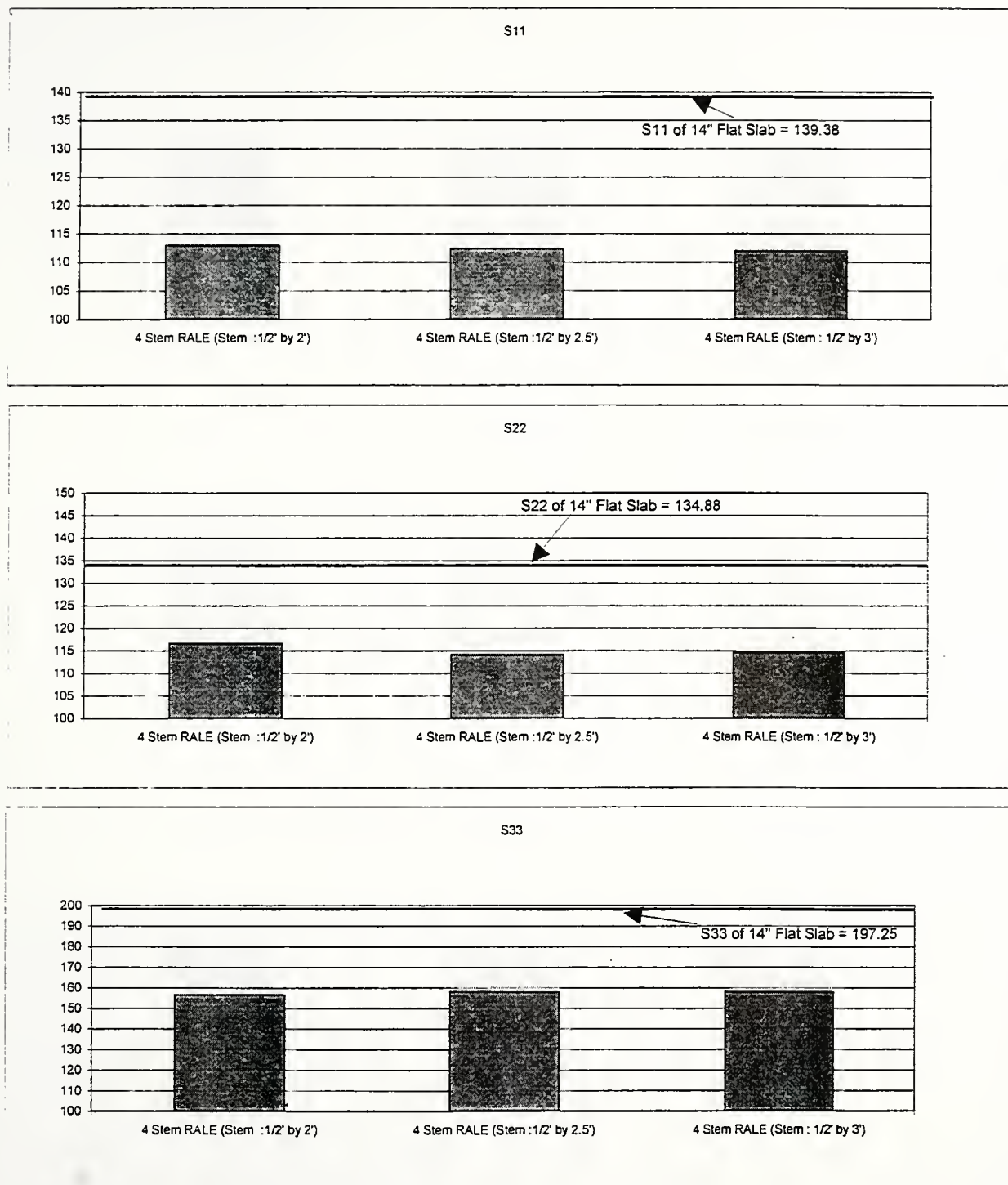


Figure 22 Comparison of conventional flat slab with different four stem RALE systems under +15C thermal load

Comparison of Flat Slab with Different Four Stem RALE Systems Under -15C Thermal Load

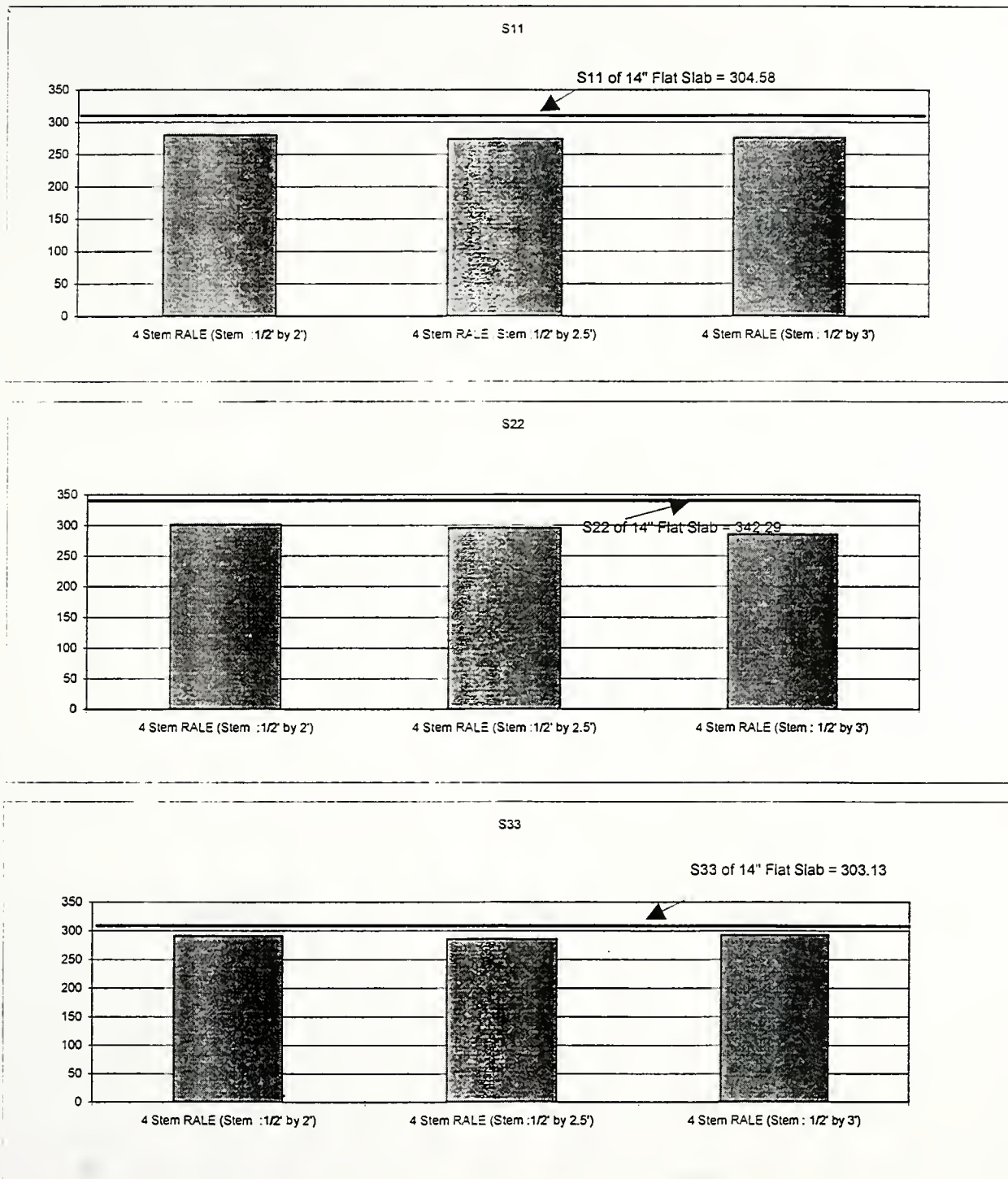


Figure 23 Comparison of conventional flat slab with different four stem RALE systems under -15C thermal load

Comparison of Flat Slab with Different Four Stem RALE Systems Under Wheel and Thermal Load +15C

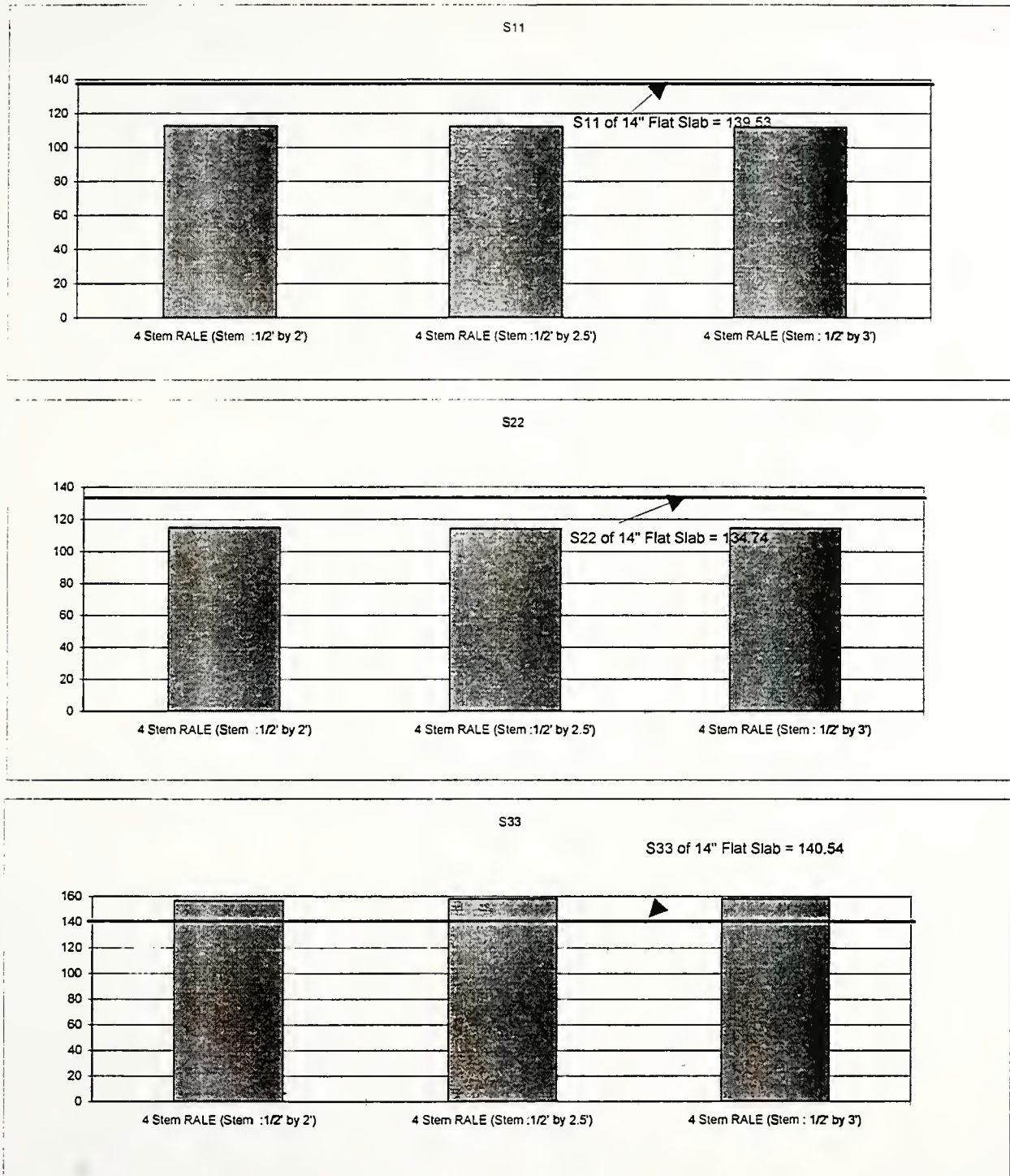


Figure 24 Comparison of conventional flat slab with different four stem RALE systems under wheel and thermal load +15C

Comparison of Flat Slab with Different Four Stem RALE Systems Under Wheel and Thermal Load -15C

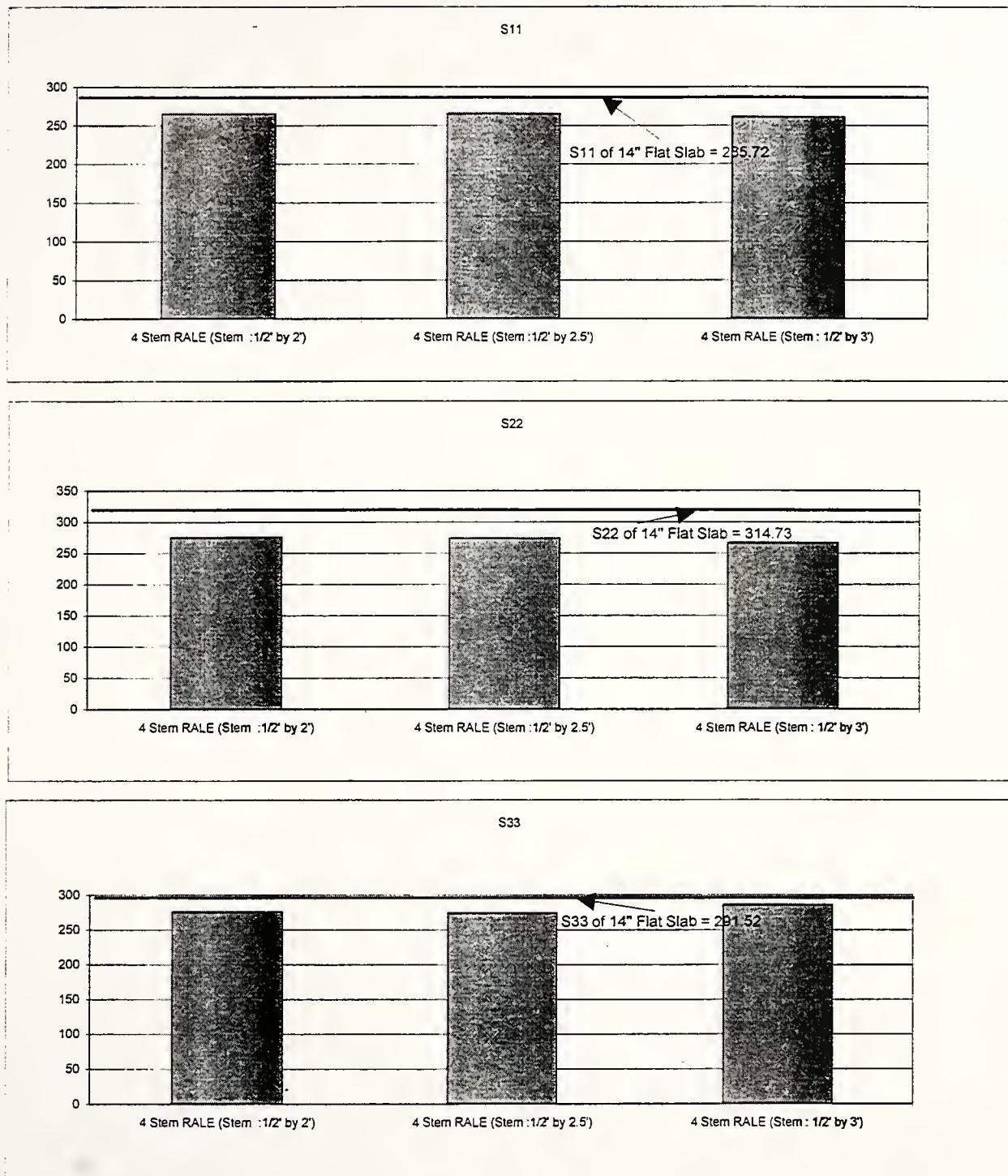


Figure 25 Comparison of conventional flat slab with different four stem RALE systems under wheel and thermal load -15C

